



myresearchspace.uws.ac.uk

Science and Art: A Future for Stone

Hughes, John; Howind, Torsten

Published: 01/01/2016

Document Version

Publisher's PDF, also known as Version of record

[Link to publication on MyResearchSpace UWS](#)

Citation for published version (APA):

Hughes, J., & Howind, T. (Eds.) (2016). Science and Art: A Future for Stone: Proceedings of the 13th International Congress on the Deterioration and Conservation of Stone, Volume 2. Paisley: University of the West of Scotland.

General rights

Copyright and moral rights for the publications made accessible in the public portal are retained by the authors and/or other copyright owners and it is a condition of accessing publications that users recognise and abide by the legal requirements associated with these rights.

- Users may download and print one copy of any publication from the public portal for the purpose of private study or research.
- You may not further distribute the material or use it for any profit-making activity or commercial gain
- You may freely distribute the URL identifying the publication in the public portal ?

Take down policy

If you believe that this document breaches copyright please contact us providing details, and we will remove access to the work immediately and investigate your claim.



SCIENCE and ART: A Future for Stone

**Proceedings of the 13th International Congress on the
Deterioration and Conservation of Stone – Volume II**

Edited by
John Hughes & Torsten Howind

LAS CASAS TAPADAS DE PLAZUELAS – STRUCTURAL DAMAGE, WEATHERING CHARACTERISTICS AND TECHNICAL PROPERTIES OF VOLCANIC ROCKS IN GUANAJUATO, MEXICO

C. Pötzl^{1*}, R.A. López-Doncel², W. Wedekind¹ and S. Siegesmund¹

Abstract

The building stones of the pyramids of Plazuelas were analysed in terms of their pore space, water transport and retention properties, as well as their mechanical properties and weathering characteristics. Based on mineralogical composition, different types of tuff could be distinguished. In a field survey the structural damages and their intensities were mapped in situ at every wall of the main building. The field investigation uncovered substantial types of damage in the used tuffs. The specimens for the laboratory investigations were prepared parallel and perpendicular to the lamination to distinguish effects of the anisotropy. The data shows that the pore space properties have the largest influence on additional rock properties (e.g. hygric expansion) of the tuffs, and hence the largest influence on the weathering resistance of the stones. Due to the local climatic conditions, some of the building stones, which would be commonly classified as unsuitable, could be classified as a proper building stone.

Keywords: tuff, weathering characteristics, technical properties, damage mapping

1. Introduction

The suitability of tuffs as building stones is strongly dependent on the environmental conditions. Therefore it is not always possible to give a general statement in terms of their application. In Mexico tuffs were used as raw material for the construction of churches, pyramids and other monuments. Due to infrastructure and availability rocks in the immediate vicinity were usually used. In the federal state of Guanajuato (Mexico) the Chichimecas, a sophisticated predecessor culture of the Aztecs that populated the adjacent Bajío region, created the pyramids of Plazuelas at approximately 450 AD (Castañeda López and Gutiérrez Lara, 2014). The central temple complex, which is also known as Casas Tapadas, consists of four pyramids and an adjacent ballgame court (Fig. 1) and is possibly connected to the worship of their gods. Because the pyramids were enlarged at least three times, one can find a minimum of three phases of construction. Around 900 AD the complex was abandoned due to a fire, which has been documented to date in the form of discoloration of the façade leaving considerable structural damages. In 1998, after the

¹ C. Pötzl*, W. Wedekind and S. Siegesmund,
Geoscience Centre of the Georg August University Göttingen, Germany,
christopher.poetzl@gmx.de

² R.A. López Doncel
Geological Institute, Autonomous University of San Luis Potosí, Mexico

*corresponding author

temple complex was buried for several centuries due to sedimentation, the Casas Tapadas were officially rediscovered and excavated in the following years.

The building stones of the pyramids experienced more than a thousand years of weathering processes and show damages and weathering characteristics equivalent to that length of time. To make sustainable and effective protection for the preservation and conservation of these valuable cultural assets, the consolidated scientific findings of the physical and mechanical properties of the building stones as well as their weathering characteristics are indispensable.

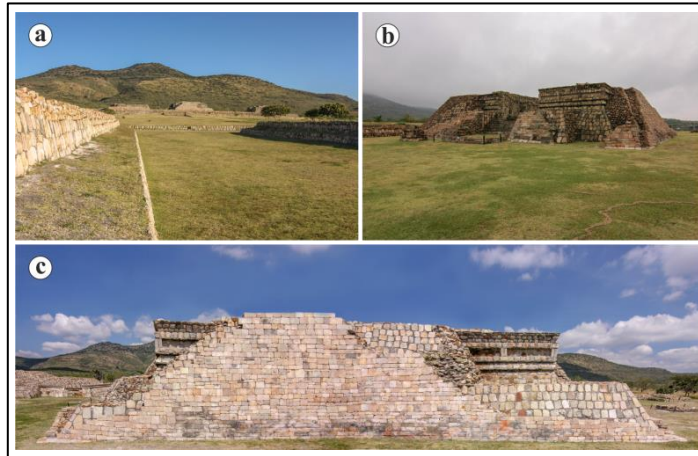


Fig. 1: a) View from the south over the ballgame court to the main pyramids; b) West side of the central pyramid with the main entrance; c) South side of the central pyramid.

2. Materials and methods

In this investigation seven different tuffs and volcanic rocks from Guanajuato were analysed. Mineralogical composition and whole rock chemistry were analysed by both optical and geochemical methods (polarized light microscopy, X-ray diffraction (XRD) and X-ray fluorescence (XRF) spectroscopy). Matrix and bulk density as well as the porosity were measured by hydrostatic weighing according to the DIN 52 102. The pore radii distribution was determined by mercury intrusion porosimetry. The capillary water absorption was measured according to DIN ISO 15148. The water vapor diffusion was measured according to DIN ISO 12572. The sorption was measured according to the DIN ISO 12571 in a climate chamber. The tensile strength measurement was determined by means of the Brazilian test. To determine the weathering behavior of the tuffs during temperature changes, a thermal expansion experiment was carried out in a climate chamber under dry and wet conditions. The moisture expansion of the rocks was determined by hydric wetting of cylindrical samples under water-saturated conditions. The specimens for the laboratory experiments were prepared parallel and perpendicular to the lamination to distinguish potential effects of anisotropy. To investigate the resistance of the rocks to salt stress, a salt-weathering test according to the DIN EN 12370 was performed. As an index of salt resistance the numbers of test-cycles were used till a 30 % of weight lost was

established. In a field survey the lithologies, the structural damages and their intensities were mapped in situ at all four sides of the main pyramid of the Casas Tapadas.

3. Results

3.1. Petrology and mineralogy

The volcanic rocks range in age from Paleogene to Quaternary (Cotler Avalos *et al.*, 2006), with chemical compositions that vary from basaltic andesite to rhyolitic tuff. The petrographic analyses of each rock sample were done on orientated thin sections under a polarization microscope (Fig.2).

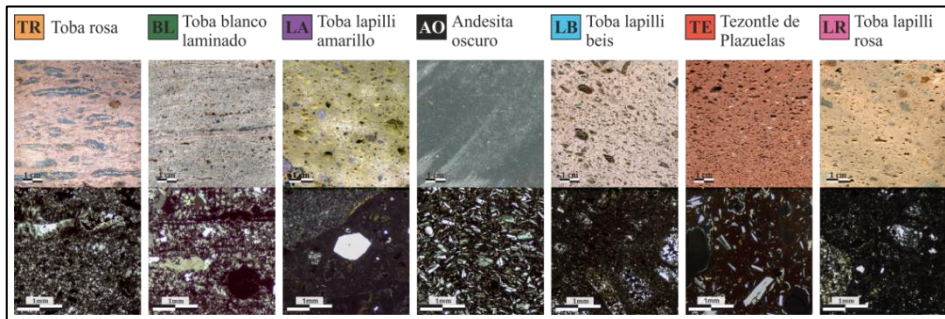


Fig. 2: Illustration of the volcanic rock samples described in detail. Top: Polished section. Bottom: Thin section under polarized light

The Toba rosa (**TR**) is a white to reddish rhyolitic tuff with grey clasts embedded in a characteristic flow texture. It mostly consists of a hypocrystalline matrix of quartz, feldspar with approximately 20 % vitric material and clasts and melting lenses up to 50 mm in length. TR is the most used rock on the pyramid. The Toba blanco laminado (**BL**) is a white to yellowish green rhyolitic tuff with a clearly recognizable lamination. Altered rocks of this type show a reddish colour. The reddish to brown clasts are less than 1 mm in size. Grey, extremely elongated clasts can be found between the layers. The Toba lapilli amarillo (**LA**) is a yellow to greenish porphyritic lapilli tuff with a dacitic composition. The proportion of clasts shows strong variations, while clasts can show sizes over 5 cm and often show andesitic composition. Variations of compact layers of ash and layers mostly consisting of clasts also occur. The rocks appear to be very porous and show many gas inclusions. It is the second most used building stone in the pyramid. The Andesita oscuro de Sierra de Penjamo (**AO**) is a microcrystalline andesite black in colour and only shows up in certain areas of the pyramid in the form of slabs of up to 5 cm of thickness. AO consists of feldspar phenocrysts with an average size of 0,2 mm with a slight orientation. The Toba lapilli beis (**LB**) is a beige porphyritic lapilli tuff with a clearly acidic composition (rhyolitic tuff). It shows slightly orientated brown clasts of pumice with sizes up to 3 cm. The Tezontle de Plazuelas (**TE**) is a red pyroclastic rock with a composition of a basaltic andesite. It appears similar to the basaltic bomb named Tezontle, which can be found nearby Mexico City. Due to many gas inclusions, the rock appears to be very porous and lightweight but strongly welded with a recognizable lamination. The Toba lapilli rosa (**LR**) is a beige to reddish rhyolitic tuff with red to brown clasts of pumice. The clasts are slightly orientated and show sizes up to 5 cm. The cryptocrystalline matrix makes up about 70 % of the rock. The volcanic lithic clasts mostly consist of feldspar.

3.2. Petrophysical properties

Whenever possible the measurements were done in three perpendicular directions of the rocks. The direction parallel to the bedding/lamination is defined as X, the direction parallel to the bedding and perpendicular to the lamination is defined as Y and the direction perpendicular to the bedding is defined as Z.

3.2.1. Pore space properties, water transport and retention properties

AO shows the lowest porosity with 0.63 vol% while having the highest bulk density with 2.73 g/cm³. TR and BL show a medium porosity of 21.1 % and 14.68 vol% and medium bulk densities of 2.05 and 2.23 g/cm³, respectively. The remaining rocks show high porosities up to 32.7 % and low bulk densities ranging between 1.56 to 1.81 g/cm³ (Tab.1). Pore radii distributions show either a unimodal distribution like AO, LB and LR or bimodal unequal like TR, BL, LA and TE (Fig.3). The amount of micropores in the rocks ranges between 9 to 85 % (Tab.1). Microporosity is defined as the pores <0.1 µm and capillary pores are defined as pores between 0.1 to 1,000 µm (Klopfen, 1985). The rock with the highest amount of micropores is LA with 85 %, followed by AO with 81 % and TR with 70 %. The remaining rocks show microporosities less than 30 % (Tab. 1).

Tab. 1: Pore space properties, moisture transport and retention properties.

Stone type	Toba rosa (TR)	Toba blanco laminado (BL)	Toba lapilli amarillo (LA)	Andesita oscuro (AO)	Toba lapilli beis (LB)	Tezontle de Plazuelas (TE)	Toba lapilli rosa (LR)
Effective porosity (vol%)	21.1	14.68	29.98	0.63	32.42	32.7	29.39
Matrix density (g/cm ³)	2.6	2.62	2.23	2.75	2.5	2.63	2.56
Bulk density (g/cm ³)	2.05	2.23	1.56	2.73	1.69	1.77	1.81
Average pore radius (µm)	0.09	0.59	0.04	0.05	0.51	2.24	0.62
Microporosity (%)	70	28	85	81	11	21	9
w value (kg/m ² √h)							
X	14.93	7.79	21.84	0.96	62.85	7.9	56.17
Y	12.41	7.13	35.87	0.99	60.5	7.9	58.36
Z	10.88	4.01	44.49	0.99	59.92	7.13	42.33
Anisotropy (%)	27	49	51	3	5	10	27
μ value							
X	41.39	32.92	14.89	58.66	18.34	18.28	14.3
Y	39.56	22.3	-	-	8.88	32.69	11.36
Z	54.72	33.26	17.51	-	13.27	63.39	14.81
Anisotropy (%)	28	33	15	-	52	71	23
max. moisture content u	0.0097	0.0054	0.0474	0.005	0.0132	0.01	0.02

The w value of the investigated rocks varies considerably. LA, LB and LR show the highest values with up to 62.85 kg/m² √h (LB). The lowest w value is shown by AO with 0.96 kg/m² √h. The w values of TR, BL and TE range between 4.01 to 14.93 kg/m² √h. The rocks show anisotropic behavior up to 51 % (Tab.1). With up to 71 % (TE) the rocks show strong anisotropic behavior of the μ value. The highest μ values are shown by TR, BL, AO and TE with up to 63.39 (TE). The remaining rocks show μ values ranging between 8.88 to 17.51. The highest u value is shown by LA with 0.0474, followed by LR with 0.02 and LB with 0.0132. The remaining rocks show u values below 0.01. The least u value is shown by AO with 0.005. Except for TE, all rocks show higher w values with rising porosity and all rocks show higher water vapor diffusion with rising porosity (Tab.1).

3.2.2. Mechanical properties

TR has the highest tensile strength with 13.23 MPa, followed by AO with 11.16 MPa. The remaining rocks show tensile strength ranging from 5.42 to 2.47 MPa (Tab.2). The tuffs show medium to high anisotropic behaviour of up to 48 % (LA). Except for TR, all rocks show lower tensile strength the higher their porosity (Tab. 1 and Tab. 2).

Tab. 2: Mechanical properties.

Stone type	Toba rosa (TR)	Toba blanco laminado (BL)	Toba lapilli amarillo (LA)	Andesita oscuro (AO)	Toba lapilli beis (LB)	Tezontle de Plazuelas (TE)	Toba lapilli rosa (LR)
Splitting tensile strength (Mpa)							
X	13.01	4.51	4.73	11.16	5.3	5.42	4.67
Y	13.23	6	4.07	-	5.2	5	4.74
Z	10.81	4.42	2.47	11.2	3.57	4.53	3.52
Anisotropy (%)	18	26	48	0	33	16	26

3.2.3. Thermal expansion, moisture expansion and salt weathering

The thermal expansion of the rocks under dry conditions shows relatively low values ranging between 0.017 to 0.028 mm/m and low anisotropies (Tab. 3). Under wet conditions the thermal expansion of TR triples, BL doubles and LA quadruples. Even the anisotropic behaviour increases up to 45 % for TR. The thermal expansion of LB, TE and LR does not change much under wet conditions (Tab. 3).

Tab. 1: Thermal expansion under dry conditions and wet conditions, hydric expansion and salt weathering.

Stone type	Toba rosa (TR)	Toba blanco laminado (BL)	Toba lapilli amarillo (LA)	Andesita oscuro (AO)	Toba lapilli beis (LB)	Tezontle de Plazuelas (TE)	Toba lapilli rosa (LR)
therm. expansion (mm/m) dry							
X	0.017	0.022	0.01	-	0.028	-	0.023
Z	0.019	0.021	0.011	0.017	0.026	0.017	0.022
Anisotropy (%)	11	5	9	-	7	-	7
therm. expansion (mm/m) wet							
X	0.0335	0.038	0.038	-	0.0275	-	0.0285
Z	0.0605	0.04	0.0425	0.024	0.03	0.0175	0.0255
Anisotropy (%)	45	5	11	-	8	-	11
hydric expansion (mm/m)							
X	0.351	0.186	0.659	-	0.057	0.085	0.007
Z	0.392	0.183	0.736	0.061	0.054	0.031	0.022
Anisotropy (%)	11	2	10	-	5	64	68
Salt weathering (cycles)	19	19	11	> 40	> 40	> 40	33

The hydric expansion of the rocks in the X and Z direction is shown in Fig. 3. It shows values that are partially multiple times higher than the thermal expansion and ranging between 0.007 mm/m for T10 and 0.736 mm/m for LA. In general the rocks show higher values for the Z direction and the anisotropy is very high for TE with 64 % and LR with 68 % (Tab.3). Every rock reaches the maximal expansion after a short time. The microporosity has a large influence on the hydric expansion (Snethlage *et al.*, 1995). In Fig. 3 we can show a good correlation of the microporosity and the hydric expansion. The

salt weathering test shows a low resistance in TR and BL with 19cycles and 11 cycles in LA until destruction. LR shows a medium resistance with 33 cycles and AO, LB and TE were not affected by salt bursting even after more than 40 cycles. Except for AO, the rocks show lower resistance against salt weathering when having a high microporosity (Tab. 1 and 3).

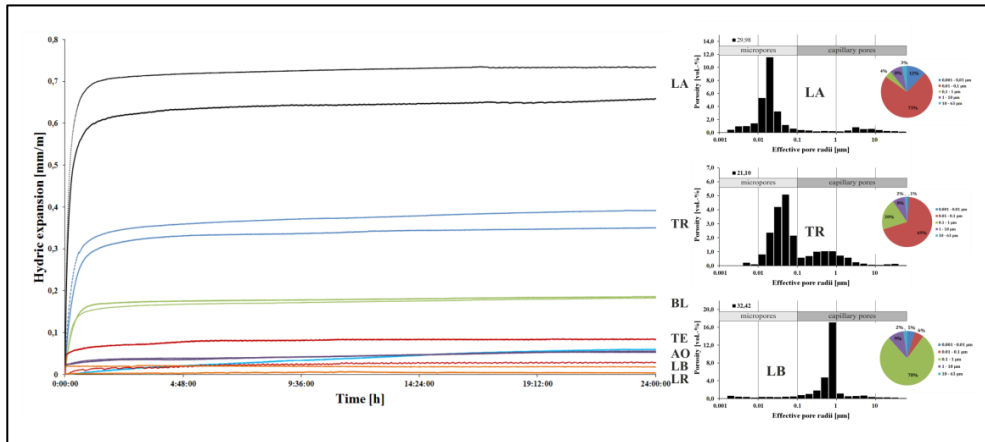


Fig. 3: Hydric expansion correlates with the microporosity on the right.

3.2.4. Salt weathering and moisture expansion related to the pore space properties

A high porosity allows the water uptake and distribution to take place and thus letting the water in the rock interact with the present clay minerals (Ruedrich *et al.*, 2011). Salt weathering is favoured due to high porosity and a bimodal pore radii distribution of the tuffs as capillary pores provides the transport for salt solutions and micropores lower the resistance of the rocks against salt crystallization. We could verify the findings from (Punuru *et al.*, 1990; Fitzner and Basten, 1994; Benavente *et al.*, 2004) that the pore radii distribution affects the stone's durability as a key factor.

3.2.5. Mapping and *in situ* investigations

Some of the main deterioration and weathering effects are caused by back weathering (Fig. 4a), fracturing (Fig. 4b), salt efflorescence (Fig. 4c) and scaling (Fig. 4d). These phenomena are often found in shady areas or areas close to the ground (Fig. 5), where water or moisture is permanently or temporarily available. The damage types were classified according to the glossary on stone and deterioration patterns of the International Scientific Committee for Stone (ISCS – ICOMOS, Anson-Cartwright, 2010). By mapping all four sides of the pyramid (Fig. 5) and combining the different lithologies with the types of damage and their intensity, we could detect the main damage sources and the building stones most susceptible to it quantitatively. Fig. 6 shows a clear correlation of increased damage intensities and an increased use of the Toba lapilli amarillo (LA) on the north and west side of the pyramid. The percentages of high to very high damage intensities can be related to LA. The rocks of the Toba rosa (TR) mostly show medium damage intensities.

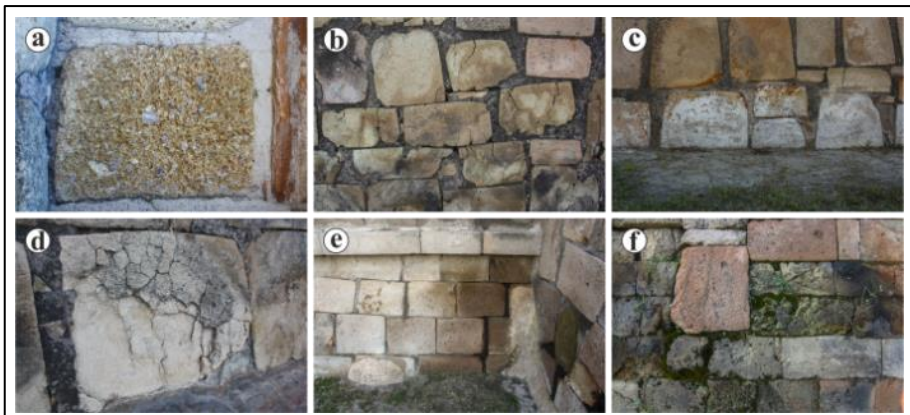


Fig. 4: Some of the main damage phenomena in the building stones of the pyramids of Plazuelas. a) Back weathering of clasts and components; b) Extensive fracturing and craquele; c) Salt efflorescence; d) Scaling; e) Discolouration due to moisture area; f) Biological colonization.

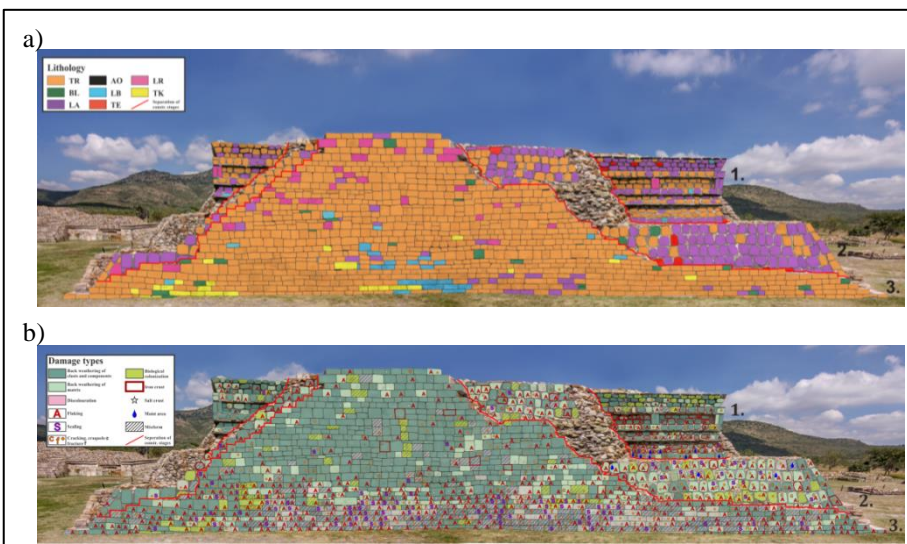


Fig. 5: Mapping of the south side of the pyramid;
a) Lithographic mapping; b) Mapping of damage types.

1 = 1st construction stage,

2 = 2nd construction stage,

3 = 3rd construction stage.

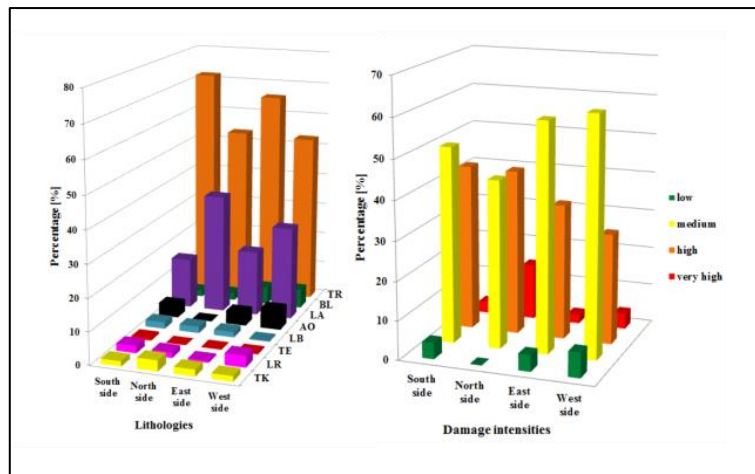


Fig. 6: Quantitative analysis of lithologies and damage intensities.

4. Conclusion

In combination with an increased hydric expansion, the rocks are in a situation where availability of water can mean both an advantage and a disadvantage. Due to precipitation the salt is washed out of the rock surface, which lowers the salt crystallization on the one hand, but increases the hydric expansion on the other hand. By comparing the distribution of the salt crusts at the different sides of the buildings clarifies how these circumstances are connected to the exposition of the building stones in the pyramid. Since the main wind direction is ESE during the rainy period, salt at the south side and east side gets washed out before it can crystallize. According to this, salt weathering only occurs in areas close to the ground where rocks can absorb the salt in solution by capillary water at any time. On the east side this process is lowered due to the influence of the wind. The north and west side of the pyramid shows an extensive distribution of salt efflorescence all over the façade due to the lack of influence from the precipitation. On the other hand, hydric expansion only occurs to a minor degree on these sides.

We were able to show that the building stones of the pyramids of Plazuelas partially suffered serious damage due to salt weathering and hydric expansion. We could approve that the pore space properties have a strong influence on the weathering behaviour of the rocks. Especially the pore radii distribution seems to play an important role. While providing a good water transport due to capillary pores as well as the availability of micropores, which lower the resistance against salt crystallization, a bimodal pore radii distribution with a high amount of micropores has proven to be inappropriate. Despite the fact that laboratory investigations show high hydric expansion and low resistance against salt weathering due to a high amount of micropores, the Toba rosa (TR) has proven to be a suitable building stone under the existing environmental conditions at the Casas Tapadas. Conservation measures will be challenged by the need of minimizing the salt contamination while facing the risk of hydric expansion.

Acknowledgements

Our work was supported by the Consejo Nacional de Ciencia y Tecnología (CONACyT), Projects Ciencia Básica (CB-130282) and Cooperación Bilateral (191044). We are grateful to G. Hartmann and K. Wemmer of the GZG for their help with the mineral analysis.

References

- Anson-Cartwright, T. (Ed.) (2010), Illustrated glossary on stone deterioration patterns: Illustriertes Glossar der Verwitterungsformen von Naturstein, Monuments and sites Monuments et sites Monumentos y sitios, Vol. 15, 1st ed., ICOMOS, International Scientific Committee for Stone (ISCS); Imhof, Paris, Petersberg.
- Benavente, D., del Cura, M.G., Fort, R. and Ordóñez, S. (2004), “Durability estimation of porous building stones from pore structure and strength”, *Engineering Geology*, Vol. 74 No. 1, pp. 113–127.
- Castañeda López, C. and Gutiérrez Lara, G. (2014), “La Arquitectura de Plazuelas”, in Viramontes Anzures, C. (Ed.), *Tiempo y Región. Estudios Históricos y Sociales: Volumen VII: Ensayos sobre cultura material entre las sociedades prehispánicas del centro-norte y occidente de México*.
- Cotler Avalos, H., Mazari Hiriart, M., Anda Sánchez, J.d., Garrido Pérez, A. and Pérez Damián, J.L. (Eds.) (2006), *Atlas de la Cuenca Lerma-Chapala: Construyendo una visión conjunta*, Instituto Nacional de Ecología, México, D.F.
- Fitzner, B. and Basten, D. (1994), “Gesteinsporosität-Klassifizierung, meßtechnische Erfassung und Bewertung ihrer Verwitterungsrelevanz”, in *Jahresberichte aus dem Forschungsprogramm Steinzerfall, Steinkonservierung*. Band 4, 1992, Ernst, Wilhelm & Sohn, Verlag für Architektur und technische Wissenschaften GmbH, Berlin, Germany, pp. 19–32.
- Klopfer, H. (1985), “Feuchte”, in Klopfer, H. (Ed.), *Lehrbuch der Bauphysik*.
- Punuru, A.R., Chowdhury, A.N., Kulshreshtha, N.P. and Gauri, K.L. (1990), “Control of porosity on durability of limestone at the Great Sphinx, Egypt”, *Environmental Geology and Water Sciences*, Vol. 15 No. 3, pp. 225–232.
- Ruedrich, J., Bartelsen, T., Dohrmann, R. and Siegesmund, S. (2011), “Moisture expansion as a deterioration factor for sandstone used in buildings”, *Environmental Earth Sciences*, Vol. 63 No. 7-8, pp. 1545–1564.
- Snethlage, R., Wendler, E. and Klemm, D.D. (1995), “Tenside im Gesteinsschutz-bisherige Resultate mit einem neuen Konzept zur Erhaltung von Denkmälern aus Naturstein”, *Denkmalpflege und Naturwissenschaft-Natursteinkonservierung I*. Verlag Ernst & Sohn, Berlin, pp. 127–146.